Journal of Molecular Catalysis A: Chemical 314 (2009) 1–9

Contents lists available at ScienceDirect

Journal of Molecular Catalysis A: Chemical

journal homepage: www.elsevier.com/locate/molcata

Editor's choice paper

Theoretical studies of stereoselectivities in the direct *anti*-Mannich and *syn*-aldol reactions catalyzed by axially chiral amino sulfonamide

Aiping Fu*, Hongliang Li, Tianshu Chu, Hanxun Zou, Peng Feng, Shuping Yuan, Yunbo Duan

Institute for Computational Science and Engineering, Laboratory of New Fiber Materials and Modern Textile, The Growing Base for State Key Laboratory, Qingdao University, Qingdao 266071, China

ARTICLE INFO

Article history:
Received 27 May 2009
Received in revised form 22 August 2009
Accepted 31 August 2009
Available online 6 September 2009

Keywords:
Syn-aldol
Anti-Mannich
Organocatalyst
Amino sulfonamide
Transition structure

ABSTRACT

The origins of the stereoselectivities in the axially chiral amino sulfonamide-catalyzed direct *anti*-Mannich and *syn*-aldol reactions have been studied with the aid of density functional theory method. Transition states of the stereochemistry-determining C–C bond-forming step with the enamine intermediate addition to the imine or aldehyde for the subject Mannich and aldol reactions are reported. BH and HLYP/6-31G** calculations provide a good explanation for the diastereoselectivities in the chiral amino sulfonamide-catalyzed *anti*-Mannich and *syn*-aldol reactions. Calculated and observed diastereomeric ratio and enantiomeric excess values are in good agreement.

1. Introduction

The direct asymmetric aldol and Mannich reactions are among the most important C–C bond-forming reactions in the construction of chiral building blocks for the synthesis of structurally complex molecules, e.g. natural products or non-natural drug molecules [1]. As a result of their great usefulness in pharmaceutical chemistry and natural product syntheses, the development of catalytic asymmetric aldol and Mannich reactions has received increased attention in recent years [1–35]. In particular, since the pioneering finding by List et al. and Barbas et al. [5–8] that proline could act as a catalyst in the direct aldol and Mannich reactions, organocatalytic direct asymmetric aldol and Mannich reactions have been a highly active research area, and thus many metal-free chiral catalysts [11–35], which include Brønsted acids [11–13], cinchona alkaloids [14–15], proline derivatives and linear amino acid derivatives [16–31], have been developed for those transformations, all attempting to reach high levels of efficiencies and to widen the scope of substrates. Although great efforts have been made to the development of efficient asymmetric aldol and Mannich reactions [3–35], most highly stereoselective strategies have been limited to the *anti*-selectivity in aldol reaction and *syn*-selectivity in the Mannich reaction. New routes which allow high enantio- and diastereo-*syn*-aldol and *anti*-Mannich reactions become to be an appealing area. Recently, Barbas' group has reported the first *syn*-selective aldol reactions between α-hydroxyketones and aromatic aldehydes catalyzed by the primary amine containing acyclic amino acid (*S*)-threonine and its derivative O^{t}Bu-(*S*)-threonine [23]. In their experiments, desired *syn*-diols were obtained with high dr (up to 18:1) and ee (up to 98% ee). Later, Gong's group has broadened the scope of the aldol donor of the Barbas' first *syn*-aldol works, and developed a new type of organocatalysts [21], which was derived from primary amino acids and β-amino alcohols, for the catalytic *syn*-selective direct aldol reactions of aldehydes with hydro-, fluoro-, and chloroacetone and 3-pentanone. They found that organic molecules derived from L-leucine and (S)-β-amino alcohols offered superior diastereo- and enantioselectivities. In fact, Barbas et al. have also explored the primary amine containing acyclic amino acid-catalyzed three-component Mannich reactions between α-hydroxyketones, aromatic aldehydes and *p*-anisidine [23]. In the experiment, the desired *anti*-Mannich products were obtained in good yields with excellent dr (up to 15:1) and ee (up to 98% ee) when primary amino acid L-tryptophan was used as catalyst. Interestingly, with respect to the *anti*-Mannich reactions [24–31], there are relatively more examples compared with the *syn*-aldol reactions [21,23]. For example, in 2002, Córdova and Barbas reported an (**S**)-2-methoxymethylpyrrolidine (SMP)-catalyzed Mannich reaction between unmodified aldehydes and N-PMP-protected α-imino ethyl glyoxylate which give the products in good yields (44–78%) with *anti*-selectivity ranging from 1:1 to >19:1 dr and good enantioselectivities (74–92% ee) [27]. Later, Jorgensen et al. [31] and Córdova et al. [28] have also reported

* Corresponding author. Fax: +86 532 85950768.
E-mail address: faplhl@eyou.com (A. Fu).

1381-1169/$ – see front matter © 2009 Elsevier B.V. All rights reserved.
doi:10.1016/j.molcata.2009.08.026

the similar catalyst of α,α-diarylprolinol siyl ether in the same direct catalytic Mannich-type reactions which afford the products with highly *anti*- and enantioselectivities. The mechanism of those organo-catalyzed *ani*-Mannich process represents the concept of the new asymmetric induction strategy and has proposed to be controlled by the efficient steric shielding instead of the commonly used hydrogen bonding concept. Very recently, Barbas's group has designed the new pyrrolidine derivatives of β-amino acid catalysts, e.g. (3*R*, 5*R*)-5-methyl-3-pyrrolidinecarboxylic acid and (*R*)-3-pyrrolidinecarboxylic acid for the *anti*-selective Mannich-type reactions of aldehydes and ketone with imine [24–26]. The *anti*-Mannich products were obtained with high stereoselectivities.

Despite the above exciting results for catalyst (**S**)-2 with amino sulfonamide functionality, an interesting change of the diastereoselectivity was also observed when switching the catalyst from (**S**)-2 to (**S**)-1, a certain artificial amino acid catalyst with the same binaphthyl backbone. As shown in Eq. (1), the direct Mannich reaction between iso-valeraldehyde and α-imino ester catalyzed by (**S**)-1 afforded the β-amino aldehyde with non-diastereoselectivity (*syn*/*anti* = 1.1/1) [32]. Moreover, (**S**)-1-catalyzed direct asymmetric aldol reaction between cyclohexanone and 4-nitrobenzaldehyde gave the *anti*-aldol adduct with excellent diastereoselectivity (*anti*/*syn* = 95:5) and good enantioselectivity (98% ee) (Eq. (3)) [34]. These intriguing phenomena call for mechanistic and theoretical investigations.

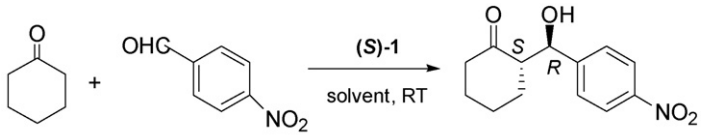

98% yield, *anti* / *syn* = 95:5, 98% ee for *anti*-isomer and 5% for *syn*-isomer. (3)

Thereafter, Córdova and coworkers have also reported the primary amine containing acyclic β^3-amino acids-catalyzed direct asymmetric *anti*-selective Mannich-type reactions between ketones and α-imino ester with high diastereo- and enantioselectivity (up to >19:1 dr, 88–99% ee) [29]. Above two experimental results indicate that the position of the carboxylic acid functionality, e.g. α or β in the amino acids catalysts directs the stereoselection of the reaction.

Besides all above important *anti*-Mannich and *syn*-aldol reactions, Maruoka and coworkers have designed a new type of axially chiral catalysts [32–34], which has a rigid and readily derivatizable binaphthyl backbone ((**S**)-1 and (**S**)-2 in Scheme 1). A highly *anti*-selective asymmetric Mannich reaction between different aldehydes and N-PMP-protected α-imino glyoxylates using a novel axially chiral amino trifluoromethanesulfonamide ((**S**)-2 in Scheme 1) as the catalyst proceeded smoothly and gave β-amino aldehydes with a high *anti*/*syn* ratio and enantioselectivity (Eq. (1)) [32].

Furthermore, although recent years have witnessed an explosive growth in the field of asymmetric organocatalysis, especially the asymmetric enamine catalysis, most of the catalysts described above relay on the same catalyst design concept, namely the replacement of the carboxylic acid group of proline with another functionality and without any modification of the "backbone" of the five-membered pyrrolidine ring [10]. Maruoka's chiral binaphthyl-based catalysts have provided a new strategy that may be utilized in the design and development of organocatalysts other than proline derivatives. Hence, the mechanism of this new type of catalyst-involved *anti*-Mannich and *syn*-aldol reactions needs theoretical investigations. It is well known that quantum mechanical calculations are an important tool in elucidating the reaction mechanism and the stereoselectivity, especially for the organo-catalyzed aldol, Mannich and other related transformations involving enamine intermediate.

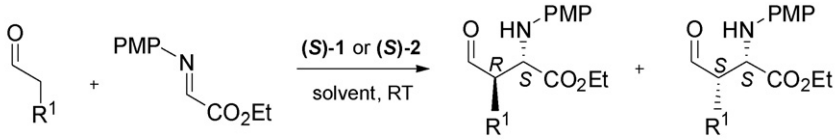

For (*S*)-1, R^1=^{i}Pr, 60% yield, *anti*: *syn* = 1:1.1, 86% ee.
For (S)-2, R^1= Me, 93% yield, *anti*: *syn* = 13:1, 99% ee; R^1=^{i}Pr, 93% yield, *anti*: *syn* = >20:1, >99% ee. (1)

Lately, they also reported the successful application of this novel axially chiral amino sulfonamide catalyst to the highly *syn*-selective and enantioselective direct cross-aldol reaction between two different aldehydes [33]. Using only 5 mol% (**S**)-2, *syn*-aldol adducts were obtained in good yields and in most cases, along with up to >20:1 diastereoselectivity and excellent enantioselectivity (92–99% ee) in all cases (Eq. (2)). This organocatalytic process represents a rare example of *syn*-selective direct cross-aldol reaction via an enamine intermediate and was complementary to the proline-catalyzed reactions with respect to the *syn*/*anti* selectivity.

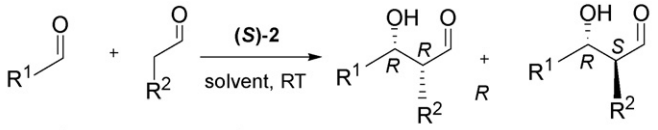

For R^1 = p-$NO_2C_6H_4$, $R^{2=}$Me, 73% yield, *syn* : *anti*= 12:1, 98% ee;
for $R^{2=}$*i* -Pr, 61% yield, *syn* : *anti*= 12:1 , 96% ee

(2)

In most cases, the diastereo- and enantioselectivity have been successfully rationalized and predicted [36–48]. To the best of our knowledge, although great effort has been made to the general understanding of the mechanism of enamine catalytic reactions [36–48], there are no other theoretical investigations concerning the *anti*-Mannich and *syn*-aldol processes involving the type of axially chiral amino sulfonamide catalyst. Hence, to extend our understanding in the mechanism and stereoselectivity of the enamine catalytic reactions, the present theoretical study is performed to explain the origin of the chiral amino sulfonamide-catalyzed *syn*-selectivity in the aldol reaction and *anti*-selectivity in the Mannich reaction.

2. Computational methods

All ground state and transition state (TS) geometries were located using density functional theory (DFT) and the BH and HLYP hybrid functional [49–50] since this functional has satisfactorily reproducing the experimental results in several organo-catalyzed Mannich reactions [51–52]. The standard 6-31G** basis sets [16]

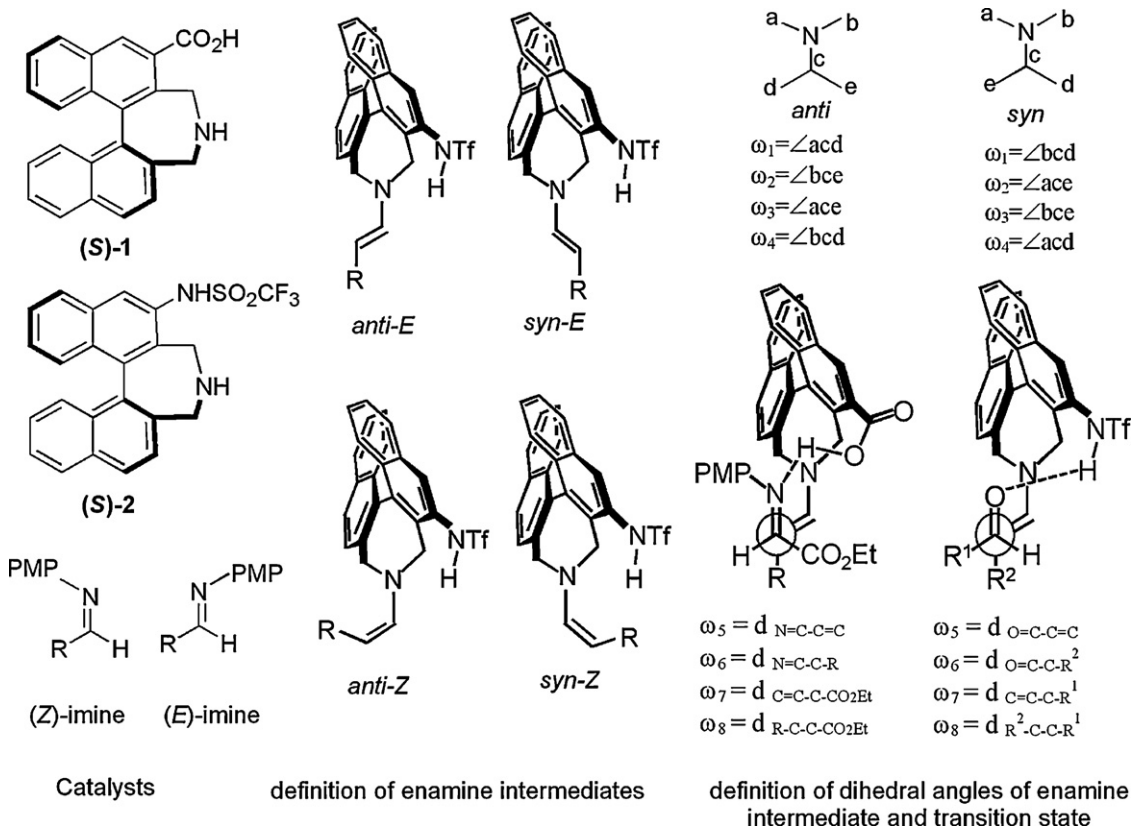

Scheme 1.

were employed throughout. All TS geometries were fully optimized and characterized by frequency analysis. The bulk effects of the solvent (DMSO for the aldol reaction and THF for the Mannich reaction) on the enamine mechanism have been taken into account by means of a dielectric continuum represented by the polarizable conductor calculation model (CPCM) [53–54], with united-atom Kohn-Sham (UAKS) radii. The single-point continuum calculations were done upon the optimized gas phase geometries with a dielectric constant $\varepsilon = 7.58$ for THF and $\varepsilon = 46.7$ for DMSO. All calculations were carried out using the Gaussian03 program [55].

3. Results and discussion

To investigate the axially chiral amino sulfonamide ((**S**)-2)-catalyzed asymmetric direct aldol and Mannich reactions which have different diastereoselectivities to those of the axially chiral amino acid ((**S**)-1)-catalyzed processes, we have used (**S**)-1 and (**S**)-2 as the prototype catalysts, and Eqs. (1)–(3) as the model reactions (for simplicity, propionaldehyde was chosen as the prototype donor in Eqs. (1) and (2)). Scheme 1 shows these catalysts and the notation used for the enamine intermediate, imine intermediate, and TSs.

Analogous to the previous investigations of the enamine-catalyzed aldol and Mannich reactions [36–48], we have focused on the TSs for the enamine attack to the imine or aldehyde. This is expected to be the stereochemistry-controlling step of the reaction and thus was studied in order to understand the observed diastereo- and enantioselectivities. Although (*Z*)-imine is computed to be more than 20 kJ/mol higher in energy than (*E*)-imine, and (*Z*)-enamines are also more than 20 kJ/mol higher in energy than their counterparts of (*E*)-enamines both for catalysts (**S**)-1 and (**S**)-2, for the sake of the full confidence to safely exclude the reactive channels involving the (*Z*)-imine and (*Z*)-enamine in the discussion of the stereoselectivities in the direct Mannich and aldol reactions, transition states for each combination of enamine and imine (*Z*/*E*, *E*/*Z*, *Z*/*Z* in addition to the most stable *E*/*E*) have been considered. As expected, those TSs involving (*Z*)-enamine and (*Z*)-imine are computed to be much higher in energy than their corresponding *E*/*E* combinations (Figs. S1–S4 in the supplementary information), and therefore, only four reactive channels corresponding to the *syn*-*E* and *anti*-*E* arrangement of the enamine double bond relative to the sulfonamide group (or carboxylic acid group), and the two diastereoisomeric approach modes to the *re* and *si* faces of (*E*)-imine or aldehyde acceptor have been further discussed in each reaction.

3.1. Anti-selective direct asymmetric Mannich reactions

Eq. (1) illustrated the *anti*-selectivity of the chiral amino sulfonamide ((**S**)-2)–catalyzed Mannich reactions involving the aldehyde and the α-imino esters, in which excellent diastereo- and enantioselectivity were obtained. In contrast, the promising axially chiral amino acid (**S**)-1 did not yield the desired major *anti*-isomer and only gave the low *syn*/*anti* selectivity (1.1/1). For the comparison purpose, we have also considered the (**S**)-1-catalyzed process.

Actually, Maruoka's *anti*-Mannich studies are based on their original hypothesis (Scheme 2): with L-proline as the catalyst, *anti*-(*E*)-enamine intermediate **A** predominates because of the steric repulsion between the enamine and acid moieties in *syn*-(*E*)-enamine. Thus, the observed *syn*-selectivity of the product can be explained by the TS involving the *anti*-(*E*)-enamine **A** attacking the *si* face of imine, which has been proposed and confirmed by Barbas [7,8], List [6], and Houk et al. [40,41] for the catalytic enantioselective Mannich reactions. While for the Maruoka's chiral organocatalyst (**S**)-1 and (**S**)-2, the authors proposed that the key for the formation of the *anti*-Mannich product is that the *syn*-(*E*)-

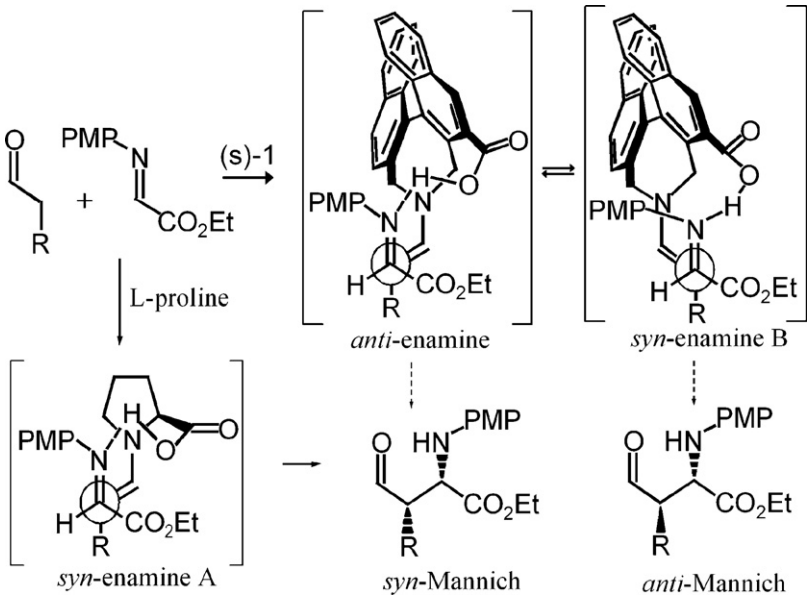

Scheme 2. A schematic representation of the proline-catalyzed *syn*-selective and (S)-1-catalyzed *anti*-selective Mannich reaction.

enamine **B** should predominate over the *anti*-(*E*)-enamine with the longer spatial distance between the amino and acid moieties in (**S**)-1 and (**S**)-2 than in the L-proline catalyst, and the imine activated by the more remote acidic proton is expected to react preferentially with the *syn*-(*E*)-enamine intermediate **B** to generate the desired *anti*-isomer.

On the basis of their design considerations, we then performed the DFT calculations on the (**S**)-1- and (**S**)-2-catalyzed Mannich reactions with propionaldehyde as the donor. The different isomers of the enamine intermediate formed between propionaldehyde and (**S**)-1 or (**S**)-2 were first explored and the relative energies between the two more stable ones (*anti*-(*E*) and *syn*-(*E*)) were small. For (**S**)-1, *syn*-(*E*)-enamine is 4.2 kJ/mol higher in energy than *anti*-(*E*)-enamine while for (**S**)-2, the former is only 1.0 kJ/mol higher than the latter. Although *anti*-(*E*) isomers are slightly more stable than the *syn*-(*E*) ones whether in the gas phase or in solution phase, there is no evidence that one isomer should be significantly preferred over the others especially for the (**S**)-2-catalyzed process.

The lowest energy TSs leading to the four stereoisomers that are *syn*- and *anti*-diastereomeric pairs of enantiomers for the stereo-controlling step of the (**S**)-1-catalyzed process have been illustrated in Fig. 1 and the corresponding TSs of the (**S**)-2-catalyzed process are shown in Fig. 2. Among the four TSs for (**S**)-1-catalyzed process, the most stable one **1a** involves the attack of the *anti*-(*E*)-enamine to the *si* face of imine, which leads to the experimentally observed major (2*S*, 3*S*)-*syn*-product. The (2*S*, 3*R*)-diastereoisomer is mainly formed through TS **1c** corresponding to the *syn*-(*E*)-enamine attacking the *si* face of imine, which lies 3.1 kJ/mol higher in energy than the most stable one **1a** in the gas phase. This energy difference decreases to 2.0 kJ/mol when the solvent effect is taken into account. Thus the observed low *syn*/*anti* ratio can be explained. The (2*R*, 3*R*)-enantiomer generated from the attack of the *syn*-(*E*)-enamine to the *re* face of imine also requires a higher energy barrier (5.9 kJ/mol in the gas phase, 7.7 kJ/mol in THF), which is in good agreement with the experimental results (86% ee). When switching the catalyst from (**S**)-1 to (**S**)-2, TS **2c** which corresponds to the addition of the *syn*-(*E*)-enamine to the *si* face of imine, changes to be the most stable one and gives the *anti*-product of (2*S*, 3*R*). The (2*S*, 3*S*)-diastereoisomer formed through TS **2a** is disfavored by 4.4 kJ/mol in the gas phase and 9.3 kJ/mol in the solution phase. Thus the high *anti*-diastereoselectivity (dr = 13:1) can be satisfactorily explained. Furthermore, the (2*R*, 3*S*)-enantiomer generated from TS **2b** requires a much higher energy barrier (26.0 kJ/mol in gas phase and 23.9 kJ/mol in THF), which is consistent with the experimental results (99% ee) [32].

Furthermore, the calculated activation energies for the C–C bond formation step relative to the imine and enamine intermediate are also given in Figs. 1 and 2. The barrier for the more favorable channel of the more acidic (**S**)-2-catalyzed process is computed to be about 26 kJ/mol smaller than those of the (**S**)-1-catalyzed process. This is in qualitative agreement with the experimentally observed increased reactivity of catalyst (**S**)-2 over (**S**)-1.

Figs. 1 and 2 also provide numerical values for several geometric parameters that are relevant for the relative stability of different TSs. These include the lengths of the forming C–C bond and the hydrogen bond, the dihedral angles ω_{1-4} that are commonly used to measure the deviation of the developing iminium bond from planarity (ideally 0°, 0°, 180°, and 180°, see Scheme 1), and the dihedral angles ω_{5-8} that represent the different arrangements of imine and enamine along the forming C–C bond (ideally ±60° and 180° for staggering conformation). As shown in Figs. 1 and 2, all of the transition states have the acidic proton completely transferred to the imine, with the forming C–C single bond having lengths of 2.20–2.35 Å. This substantial ionic interaction between an iminium and the COO^- or TfN^-- is the common feature of the proline-catalyzed Mannich reactions proposed by Houk's group [40,41]. The C–C lengths at the (**S**)-2-catalyzed process are slightly longer than those associated with the (**S**)-1-catlyzed one. In addition, the hydrogen bond lengths of NH···N at the (**S**)-2-catalyzed process are much longer than those of the NH···O involved in the (**S**)-1-catalyzed one. As has been pointed out in the previous proline and its derivatives-catalyzed aldol and Mannich process [36–48], the following factors may contribute to the enantioselectivity and diastereoselectivity. First, the stereoselectivity partially arises from the different degrees to which each diastereomeric transition states satisfies iminium planarity. Generally, the more stable TS is always associated with a "more planar" iminum moiety. Comparing the dihedral angles ω_{1-4} of TS **2a**–**2c** illustrated in Fig. 2 with their counterparts of **1a**–**1c** in Fig. 1, we can see that there is more out-of-plane deformation of iminium in **2a** and **2b** than those in **1a** and **1b**. This may ultimately determine the relative energies of the various TSs and make **2c** being preferred over **2a**, which then sub-

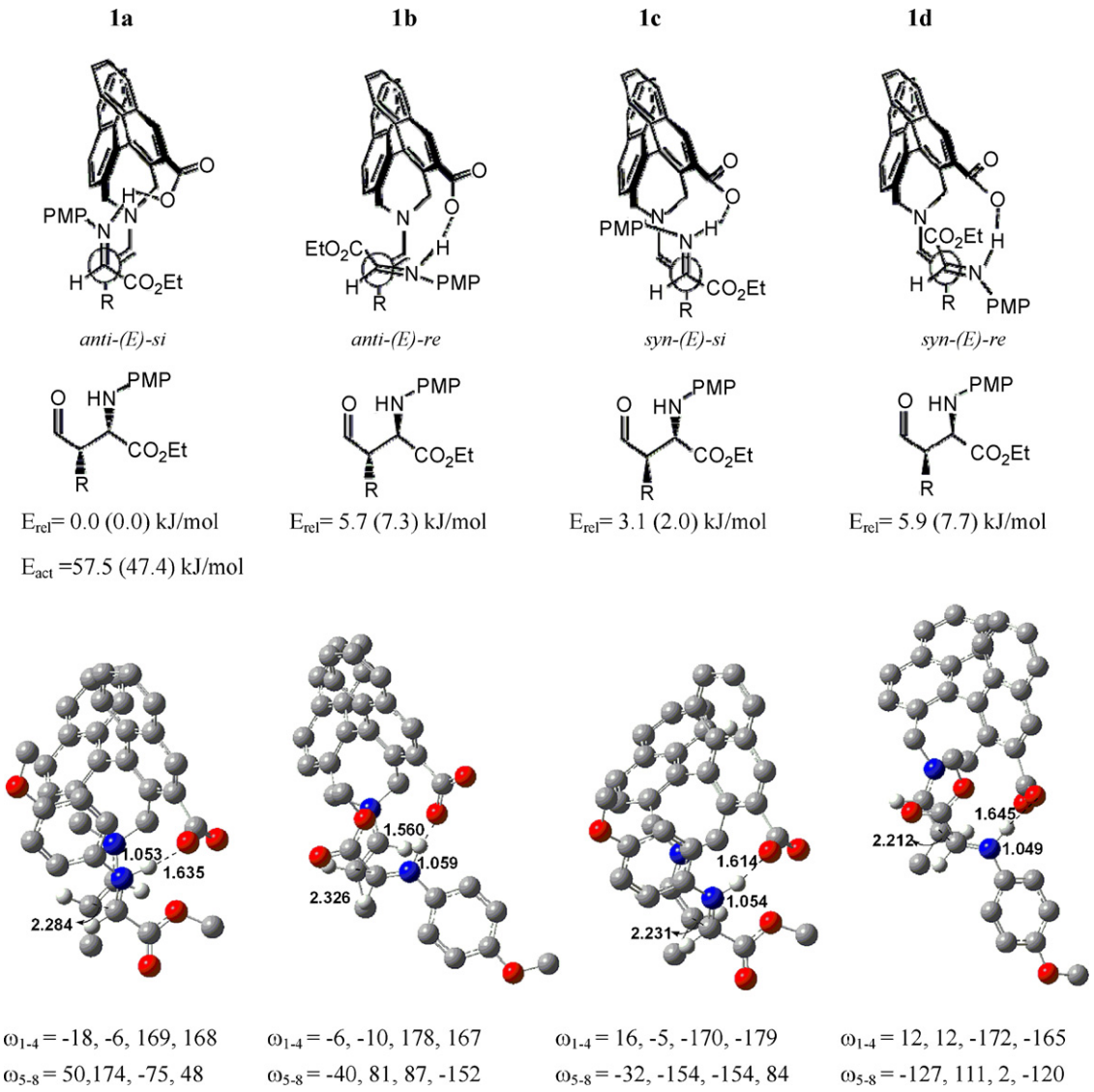

Fig. 1. Transition structures and relative energies at BH and HLYP/6-31G** level for the C–C bond formation step of the (**S**)-1-catalyzed Mannich reaction between propionaldehyde and N-PMP-protected α-imino methyl glyoxylate. Values in parentheses including solvation energies in THF using the CPCM/UAKS model. E_{act} is the activation energy relative to the imine and *anti*-enamine. Different TS arrangements of imine and enamine along the forming C–C bond that generate the four diastereoisomers are shown. For clarity, some of the hydrogen atoms at the periphery are omitted.

sequently switch the diastereoselectivity from low *syn*/*anti* ratio in the (**S**)-1 catalyzed process to high *anti*-selectivity in the (**S**)-2-catalyzed one. The second factor that regulates the stereoselectivity is the different arrangements of imine and enamine along the forming C–C bond. Of course, intermolecular hydrogen bonding and steric repulsion may change the ideal arrangement from the staggering to the more eclipsed ones (ω_{5-8} shown in Scheme 1 and Figs. 1 and 2). However, TSs with the more staggering orientation at the reaction center should be preferred over the other ones. These factors combine to affect the relative energies of the various TSs and subsequently the stereoselectivity. In summary, the origin of the different diastereoselectivities in the direct Mannich reactions when the flexible carboxylic acid functionality of (**S**)-1 was replaced by the rigid and distant trifluoromethanesulfonamide group can be explained as the direct consequence of the different spatial distance between amino and the acid group of the two catalysts leading to two different TSs. In the (**S**)-1 catalyzed process, the flexibility of the carboxylic acid group allows the imine to react via both the *anti*-(*E*)-enamine and *syn*-(*E*)-enamine, giving rise to roughly equal amounts of both *anti*- and *syn*-isomers. In contrast, the rigid and more remote acidic proton in (**S**)-2 results in the large distortions of the developing iminium from planarity in the reaction of the imine approaching the *anti*-(*E*)-enamine to achieve the proton transfer, directs the reaction mainly involving the *syn*-(*E*)-enamine attacking the *si* face of imine and makes the *anti*-isomer to be favored. Our calculated results satisfactorily support Maruoka's design considerations.

3.2. *Syn*-selective direct asymmetric aldol reactions

As shown in Eq. (2), Maruoka et al. have reported the highly *syn*-selective and enantioselective direct cross-aldol reactions between two different aldehydes using chiral amino sulfonamide (**S**)-2 as the catalyst [33]. Furthermore, in their previous work, they have also reported the successful application of axially chiral amino acid catalyst (**S**)-1 to the direct asymmetric aldol reaction between cyclohexanone and 4-nitrobenzaldehyde which provide *anti*-products in good yields and excellent enantioselectivities (as shown in Eq. (3)).

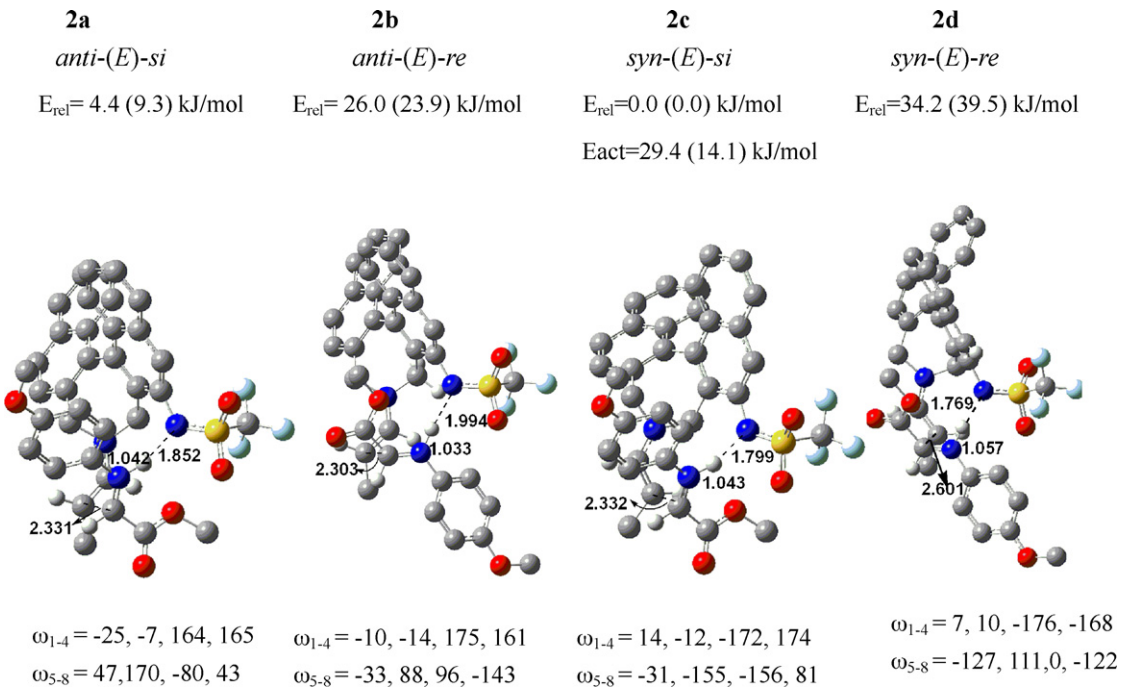

Fig. 2. Transition structures and relative energies at BH and HLYP/6-31G** level for the C–C bond formation step of the (**S**)-2-catalyzed Mannich reaction between propionaldehyde and N-PMP-protected α-imino methyl glyoxylate. Values in parentheses including solvation energies in THF using the CPCM/UAKS model. E_{act} is the activation energy relative to the imine and *anti*-enamine. For clarity, some of the hydrogen atoms at the periphery are omitted.

Based on the observation of the direct *anti*-Mannich reactions, the authors explained the observed (**S**)-2-catalyzed *syn*-selectivity with the help of Scheme 3, where the hydrogen bonding activation of the acceptor aldehyde by the acidic proton of triflamide directs the reaction to proceed via the *syn*-(*E*)-enamine intermediate. In consequence, chiral amino sulfonamide catalyst (**S**)-2 will give the *syn*-product predominantly, which is a minor diastereomer in the proline-catalyzed reaction. By contrast, the *anti*-selective reaction shown in Eq. (3) between aldehyde and cyclohexanone in the presence of axially chiral amino acid catalyst (**S**)-1 mainly proceeds via the *re* face of aldehyde attacking the *anti*-(*E*)-enamine, similar to the TS in the proline-catalyzed reaction.

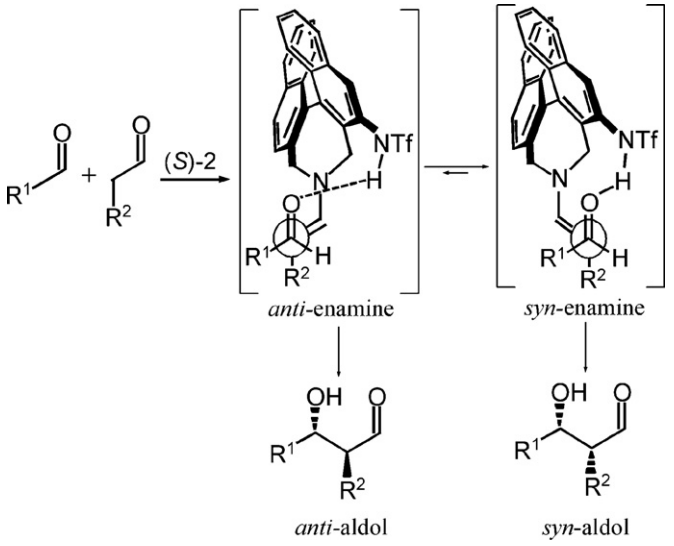

Scheme 3. A schematic representation of the (**S**)-2-catalyzed *syn*-selective aldol reaction.

Based on their design considerations, we also performed the DFT calculations on TSs for the enamine attack to the aldehyde in the C–C bond formation step of the (**S**)-1 and (**S**)-2 catalyzed aldol reactions shown in Eqs. (2) and (3). In order to evaluate the different effect of catalysts (**S**)-2 and (**S**)-1 in the same reaction, we have also considered the aldol reaction between propionaldehyde and 4-nitrobenzaldehyde in the presence of (**S**)-1.

Fig. 3 shows the four lower energy TSs that generate the four different stereoisomers for the direct aldol reaction between propionaldehyde and 4-nitrobenzaldehyde catalyzed by (**S**)-2. The corresponding four TSs for the (**S**)-1 catalyzed process are illustrated in Fig. 4. In addition, four TSs for the reaction between cyclohexanone and 4-nitrobenzaldehyde catalyzed by (**S**)-1 are presented in Fig. 5.

Among the four TSs shown in Fig. 3, as expected, **3c** involving the *re* face of aldehyde attacking *syn*-(*E*)-enamine, requires the lowest activation energy and leads to the experimentally observed major (2*R*, 3*R*)-*syn*-product, which is the minor diastereomer in the proline-catalyzed reaction. The (2*R*, 3*S*)-diastereomer is formed through TS **3d** corresponding to the *syn*-(*E*)-enamine attacking the *si* face of aldehyde, which lies 7.0 kJ/mol higher in energy than the most stable one **3c** in the gas phase. This energy difference decreases to 5.5 kJ/mol when the solvent effect is taken into account. Thus the high *syn*-diastereoselectivity (dr = 12:1) can be explained. The (2*S*, 3*S*)-enantiomer generated from the attack of *anti*-(*E*)-enamine to the *si* face of aldehyde also requires a higher energy barrier (20.8 kJ/mol in the gas phase, 20.7 kJ/mol in DMSO), which is in good agreement with the experimental results (98% ee) [33]. For the (**S**)-1-catalyzed process as shown in Figs. 4 and 5, whether for the reaction using propionaldehyde or cyclohexanone as the aldol donor, the most favorable TS involves the *anti*-(*E*)-enamine approaching the *re* face of aldehyde (TS **4a** and **5a**), which leads to the experimentally observed major product of *anti*-selectivity. The *syn*-diastereoisomer requires a higher energy barrier (8.4(4.4) kJ/mol for propionaldehyde donor and 18.4(13.4) kJ/mol for cyclohexanone donor), thus reasonably explaining the high *anti*/*syn* diastereoselectivity observed in Eq. (3)

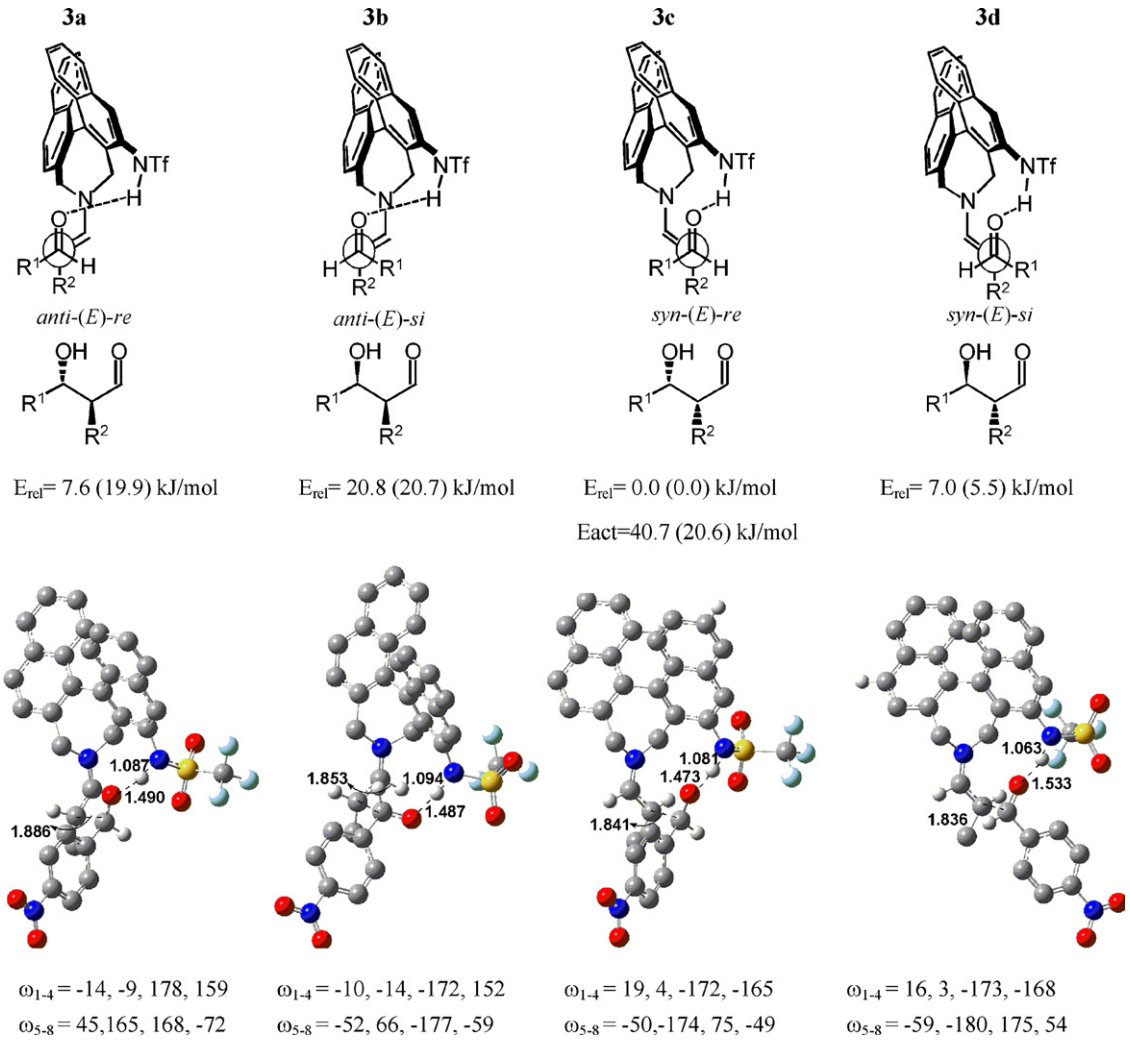

Fig. 3. Transition structures and relative energies at BH and HLYP/6-31G** level for the C–C bond formation step of the (**S**)-2-catalyzed aldol reaction between propionaldehyde and 4-nitrobenzyaldehyde. Values in parentheses including solvation energies in DMSO using the CPCM/UAKS model. E_{act} is the activation energy relative to the aldehyde and *anti*-enamine. Different TS arrangements of aldehyde and enamine along the forming C–C bond that generate the four diastereoisomers are shown. For clarity, some of the hydrogen atoms at the periphery are omitted.

using cyclohexanone as the aldol donor. The (2*S*, 3*S*)-enantiomer is formed through TS **5d** for the reaction of Eq. (3), which lies about 31 kJ/mol higher in energy than that of **5a**. This is in qualitative agreement with the experimental ee value (98% ee) [34].

Moreover, the calculated activation energies for the C–C bond formation step relative to the aldehyde and enamine intermediate are also shown in Figs. 3 and 4. As expected, the barrier for the more favorable channel is lowered when switching the catalyst from (**S**)-1 to (**S**)-2. This also suggests the increased reactivity of the more acidic (**S**)-2 over (**S**)-1 in the direct aldol reaction.

The origin of the opposite *syn* versus *anti* diastereoselectivities in the (**S**)-2 and (**S**)-1-catalyzed aldol reactions can also be explained by scrutiny of the geometrical arrangements of the TSs (shown in Figs. 3–5). As has been pointed out in the previous proline and its derivatives-catalyzed aldol and Mannich process [36–48], the different degrees to which each diastereomeric transition state satisfies iminium planarity (ω_{1-4}), and the different arrangements adopted by enamine and aldehyde along the forming C–C bond (ω_{5-8}) combine to affect the enantioselectivity and diastereoselectivity. Comparing Fig. 3 with Figs. 4 and 5, we can see that there is large distortion of the iminium moiety of the TSs involving *syn*-(*E*)-enamine (TS **4c**, **4d**, **5c**, and **5d**) in the (**S**)-1-catalyzed processes than the (**S**)-2-catalyzed one (TS **3c** and **3d**). This distortion determines the relative energies of different TSs and switch the diastereoselectivity from *anti* in the (**S**)-1-catlyzed process to *syn* in the (**S**)-2-catalyzed one.

In summary, whether in the axially chiral amino acid (**S**)-1 and axially chiral amino sulfonamide (**S**)-2-catalyzed direct Mannich reactions, or the (**S**)-1 and (**S**)-2 catalyzed direct aldol reactions, the change of the diastereoselectivity was both observed when the carboxylic acid functionality of (**S**)-1 was replaced by the sulfonamide group in (**S**)-2. These results indicate that the tuning of the proper distance between the amino group and the acid moiety in the catalyst makes a significant effect in directing the stereochemical outcome of the reaction. The key for the *syn*-aldol and *anti*-Mannich product is that the TS involving *syn*-(*E*)-enamine predominates over those involving *anti*-(*E*)-enamine in the C–C bond-forming step since the nucleophilic carbon of enamine is properly positioned to react with the aldehyde or imine when the more remote proton transfer occurs from the sulfonamide group to the oxygen or nitrogen atom of the electrophile. While in the (**S**)-1-catalyzed aldol and Mannich reaction, the major products generate from the TS involving *anti*-(*E*)-enamine, similar to the proline-catalyzed processes.

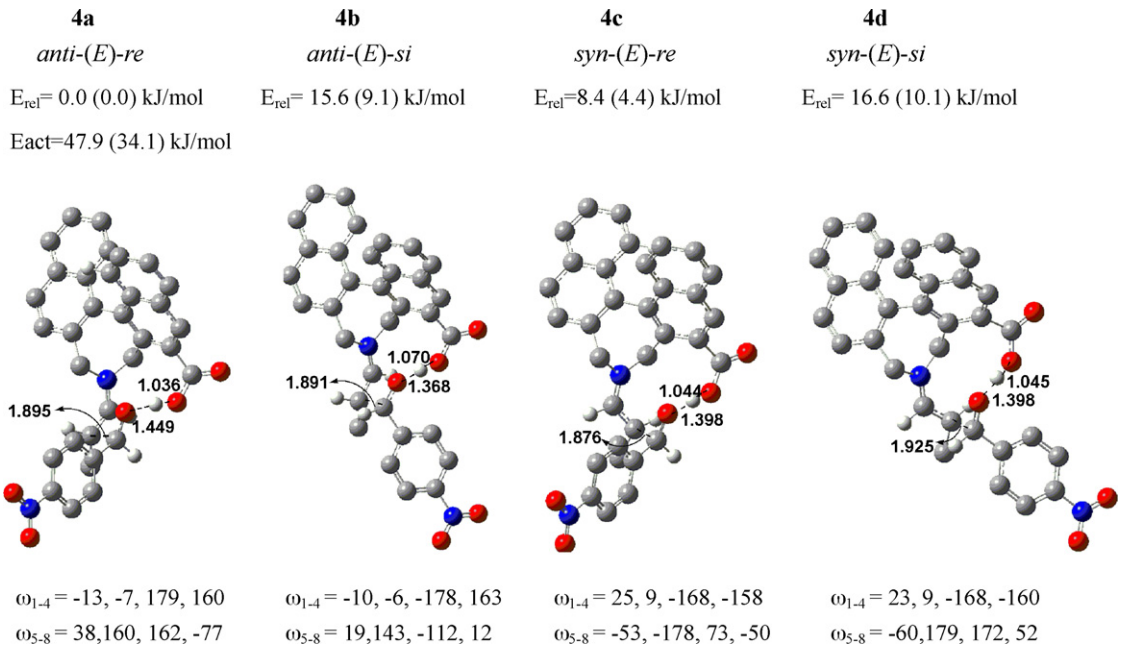

Fig. 4. Transition structures and relative energies at BH and HLYP/6-31G** level for the C–C bond formation step of the (**S**)-1-catalyzed aldol reaction between propionaldehyde and 4-nitrobenzyaldehyde. Values in parentheses including solvation energies in DMSO using the CPCM/UAKS model. E_{act} is the activation energy relative to the aldehyde and *anti*-enamine. For clarity, some of the hydrogen atoms at the periphery are omitted.

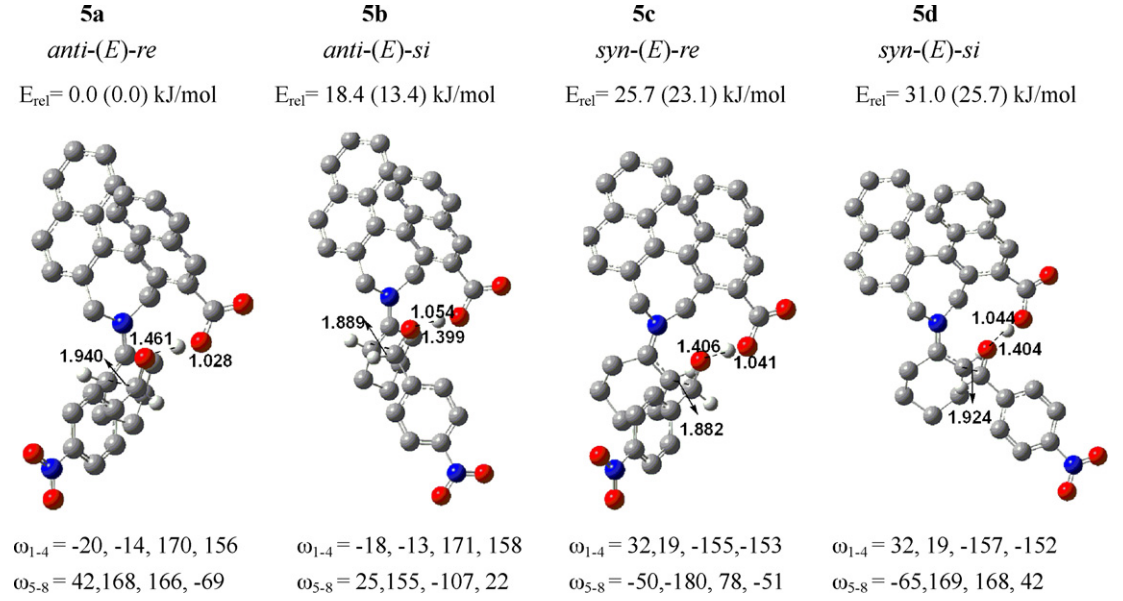

Fig. 5. Transition structures and relative energies at BH and HLYP/6-31G** level for the C–C bond formation step of the (**S**)-1-catalyzed aldol reaction between cyclohexanone and 4-nitrobenzyaldehyde. Values in parentheses including solvation energies in DMSO using the CPCM/UAKS model. E_{act} is the activation energy relative to the aldehyde and *anti*-enamine. For clarity, some of the hydrogen atoms at the periphery are omitted.

4. Conclusions

The transition structures associated with the C–C bond formation step of the axially chiral amino acid (**S**)-1 and axially chiral amino sulfonamide (**S**)-2-catalyzed direct aldol and Mannich reactions have been studied using BH and HLYP method at the 6-31G** basis set level. Our calculations confirm that the different diastereoselectivities found with the catalysts (**S**)-1 and the (**S**)-2 arise from the different structures of the TSs. The flexible carboxylic acid group in (**S**)-1 directs the reaction proceed through *anti*-(*E*)-enamine intermediate, which yield the *anti*-aldol and *syn*-Mannich products similar to the proline-catalyzed process, while the more remote and rigid trifluoromethanesulfonamide group in (**S**)-2 makes the reaction occur through *syn*-(*E*)-enamine intermediate and alters the diastereoselectivities. Our calculations confirm the idea that tuning the proper distance between the amino group and the acid moiety in the catalyst can control the main reaction channels and subsequently the stereoselectivities. This is a very useful strategy to achieve different isomers in the asymmetric synthesis process.

Acknowledgements

This work was supported by the National Natural Science Foundation of China (Nos: 20773071, 50602028, and 10874096). We also

thank the Qingdao University Research Fund for Financial Support (063-06300506).

Appendix A. Supplementary data

Supplementary data associated with this article can be found, in the online version, at doi:10.1016/j.molcata.2009.08.026.

References

[1] C.H. Heathcock, in: B.M. Trost, I. Fleming, C.H. Heathcock (Eds.), Comprehensive Organic Synthesis, 2, Pergamon Press, Oxford, 1991.
[2] M. Arend, B. Westermann, N. Risch, Angew. Chem., Int. Ed. 37 (1998) 1044–1070.
[3] B.M. Trost, Science 254 (1991) 1471–1477.
[4] C.F. Barbas III, A. Heine, G. Zhong, T. Hoffmann, S. Gramatikova, R. Björnestedt, B. List, J. Anderson, E.A. Stura, I.A. Wilson, R.A. Lerner, Science 278 (1997) 2085–2092.
[5] B. List, R.A. Lerner, C.F. Barbas III, J. Am. Chem. Soc. 122 (2000) 2395–2396.
[6] B. List, J. Am. Chem. Soc. 122 (2000) 9336–9337.
[7] A. Córdova, S.-I. Watanabe, F. Tanaka, W. Notz, C.F. Barbas III, J. Am. Chem. Soc. 24 (2002) 1866–1867.
[8] A. Córdova, W. Notz, G. Zhong, J.M. Betancort, C.F. Barbas III, J. Am. Chem. Soc. 124 (2002) 1842–1843.
[9] A.B. Northrup, D.W.C. MacMillan, J. Am. Chem. Soc. 124 (2002) 6798–6799.
[10] S. Mukherjee, J.-W. Yang, S. Hoffmann, B. List, Chem. Rev. 107 (2007) 5471–5569.
[11] T. Akiyama, J. Itoh, K. Yokota, K. Fuchibe, Angew. Chem., Int. Ed. 43 (2004) 1566–1568.
[12] D. Uraguchi, M. Terada, J. Am. Chem. Soc. 126 (2004) 5356–5357.
[13] Q.-X. Guo, H. Liu, C. Guo, S.-W. Luo, Y. Gu, L.-Z. Gong, J. Am. Chem. Soc. 129 (2007) 3790–3791.
[14] S. Lou, B.M. Taoka, A. Ting, S. Schaus, J. Am. Chem. Soc. 127 (2003) 11256–11257.
[15] A.L. Tillman, J. Ye, D.J. Dixon, Chem. Commun. (2006) 1191–1193.
[16] A. Hartikka, P.I. Arvidsson, Tetrahedron: Asymm. 15 (2004) 1831–1834.
[17] H. Torii, M. Nakadai, K. Ishihara, S. Saito, H. Yamamoto, Angew. Chem., Int. Ed. 43 (2004) 1983–1986.
[18] A. Berkessel, B. Koch, J. Lex, Adv. Synth. Catal. 346 (2004) 1141–1146.
[19] Z. Tang, F. Jiang, L.-T. Yu, X. Cui, L.-Z. Gong, A.-Q. Mi, Y.-Z. Jiang, Y.-D. Wu, J. Am. Chem. Soc. 125 (2003) 5262–5263.
[20] Z. Tang, Z.-H. Yang, X.-H. Chen, L.-F. Cun, A.-Q. Mi, Y.-Z. Jiang, L.-Z. Gong, J. Am. Chem. Soc. 127 (2005) 9285–9286.
[21] X.Y. Xu, Y.Z. Wang, L.Z. Gong, Org. Lett. 9 (2007) 4247–4249.
[22] A.J.A. Cobb, D.M. Shaw, S.V. Ley, Synlett (2004) 558–560.
[23] S.S.V. Ramasastry, H. Zhang, F. Tanaka, C.F. Barbas III, J. Am. Chem. Soc. 129 (2007) 288–289.
[24] S. Mitsumori, H. Zhang, P.H.-Y. Cheong, K.N. Houk, F. Tanaka, C.F. Barbas III, J. Am. Chem. Soc. 128 (2006) 1040–1041.
[25] H. Zhang, M. Mifsud, F. Tanaka, C.F. Barbas III, J. Am. Chem. Soc. 128 (2006) 9630–9631.
[26] H. Zhang, S. Mitsumori, N. Utsumi, M. Imai, N. Garcia-Delgado, M. Mifsud, K. Albertshofer, P.H.-Y. Cheong, K.N. Houk, F. Tanaka, C.F. Barbas III, J. Am. Chem. Soc. 130 (2008) 875–886.
[27] A. Córdova, C.F. Barbas III, Tetrahedron Lett. 43 (2002) 7749–7752.
[28] I. Ibrahem, A. Córdova, Chem. Commun. (2006) 1760–1762.
[29] P. Dziedzic, A. Córdova, Tetrahedron: Asymm. 18 (2007) 1033–1037.
[30] L. Cheng, X. Han, H. Huang, M.W. Wong, Y. Lu, Chem. Commun. (2007) 4143–4145.
[31] J. Franzen, M. Marigo, D. Fielenbach, T.C. Wabnitz, A. Kjaersgaard, K.A. Jorgensen, J. Am. Chem. Soc. 127 (2005) 18296–18304.
[32] T. Kano, Y. Yamaguchi, O. Tokuda, K. Maruoka, J. Am. Chem. Soc. 127 (2005) 16408–16409.
[33] T. Kano, Y. Yamaguchi, Y. Tanaka, K. Maruoka, Angew. Chem., Int. Ed. 46 (2007) 1738–1740.
[34] T. Kano, O. Tokuda, J. Takai, K. Maruoka, Chem. Asian J. 1–2 (2006) 210–215.
[35] T. Kano, Y. Hato, A. Yamamoto, K. Maruoka, Tetrahedron 64 (2008) 1197–1203.
[36] S. Bahmanyar, K.N. Houk, J. Am. Chem. Soc. 123 (2001) 11273–11283.
[37] S. Bahmanyar, K.N. Houk, H.J. Martin, B. List, J. Am. Chem. Soc. 125 (2003) 2475–2479.
[38] C. Allemann, R. Gordillo, F.R. Clemente, P.H. Cheong, K.N. Houk, Acc. Chem. Res. 37 (2004) 558–569.
[39] F.R. Clemente, K.N. Houk, J. Am. Chem. Soc. 127 (2005) 11294–11300.
[40] S. Bahmanyar, K.N. Houk, Org. Lett. 5 (2003) 1249–1251.
[41] P.H.-Y. Cheong, H. Zhang, R. Thayumanavan, F. Tanaka, K.N. Houk, C.F. Barbas III, Org. Lett. 8 (2006) 811–814.
[42] K.N. Rankin, J.W. Gauld, R.J. Boyd, J. Phys. Chem. A 106 (2002) 5155–5159.
[43] M. Arno, L.R. Domingo, Theor. Chem. Acc. 108 (2002) 232–239.
[44] M. Arno, R.J. Zaragoza, L.R. Domingo, Tetrahedron: Asymm. 16 (2005) 2764–2770.
[45] M. Arno, R.J. Zaragoza, L.R. Domingo, Tetrahedron: Asymm. 18 (2007) 157–164.
[46] A. Bassan, W. Zou, E. Reyes, F. Himo, A. Córdova, Angew. Chem., Int. Ed. 44 (2005) 7028–7032.
[47] P. Hammar, A. Córdova, F. Himo, Tetrahedron: Asymm. 19 (2008) 1617–1621.
[48] H.L. Li, A.P. Fu, H.N. Shi, J. Mol. Catal. A: Chem. 303 (2009) 1–8.
[49] A.D. Becke, J. Chem. Phys. 98 (1993) 5648–5652.
[50] A.D. Becke, J. Chem. Phys. 98 (1993) 1372–1377.
[51] M. Yamanaka, J. Itoh, K. Fuchibe, T. Akiyama, J. Am. Chem. Soc. 129 (2007) 6756–6764.
[52] A.P. Fu, H.L. Li, H.Z. Si, S.P. Yuan, Y.B. Duan, Tetrahedron: Asymm. 19 (2008) 2285–2292.
[53] V. Barone, M. Cossi, J. Phys. Chem. A 102 (1998) 1995–2001.
[54] B. Barone, M. Cossi, J. Tomasi, J. Comput. Chem. 19 (1998) 404–417.
[55] M.J. Frisch, G.W. Trucks, H.B. Schlegel, G.E. Scuseria, M.A. Robb, J.R. Cheeseman, J.A. Montgomery, T. Vreven, K.N. Kudin, J.C. Burant, J.M. Millam, S.S. Iyengar, J. Tomasi, V. Barone, B. Mennucci, M. Cossi, G. Scalmani, N. Rega, G.A. Petersson, H. Nakatsuji, M. Hada, M. Ehara, K. Toyota, R. Fukuda, J. Hasegawa, M. Ishida, T. Nakajima, Y. Honda, O. Kitao, H. Nakai, M. Klene, X. Li, J.E. Knox, H.P. Hratchian, J.B. Cross, C. Adamo, J. Jaramillo, R. Gomperts, R.E. Stratmann, O. Yazyev, A.J. Austin, R. Cammi, C. Pomelli, J.W. Ochterski, P.Y. Ayala, K. Morokuma, G.A. Voth, P. Salvador, J.J. Dannenberg, V.G. Zakrzewski, S. Dapprich, A.D. Daniels, M.C. Strain, O. Farkas, D.K. Malick, A.D. Rabuck, K. Raghavachari, J.B. Foresman, J.V. Ortiz, Q. Cui, A.G. Baboul, S. Clifford, J. Cioslowski, B.B. Stefanov, G. Liu, A. Liashenko, P. Piskorz, I. Komaromi, I.L. Martin, D.J. Fox, T. Keith, M.A. Al-Laham, C.Y. Peng, A. Nanayakkara, M. Challacombe, P.M.W. Gill, B. Johnson, W. Chen, M.W. Wong, C. Gonzales, J.A. Pople, Gaussian03, Revision D. 01, Gaussian, Inc., Wallingford, CT, 2004.